

Facile Synthesis of Calcium Hydroxide Nanoparticles onto TEMPO-Oxidized Cellulose Nanofibers for Heritage Conservation

Mounir El Bakkari, Vivek Bindiganavile, and Yaman Boluk*

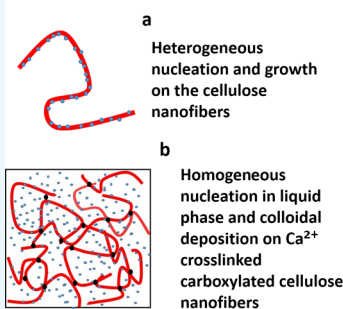
Department of Civil and Environmental Engineering, University of Alberta, Edmonton, AB T6G 2W2, Canada

Supporting Information

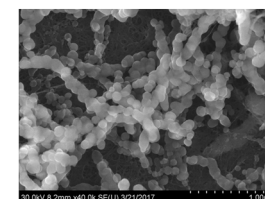
ABSTRACT: Calcium hydroxide is used in diverse applications including heritage conservation where supplying it in the form of nanoparticles allows easy carbonation with atmospheric air contacts. The effects of cellulose nanofibers on the precipitation of calcium hydroxide nanoparticles were investigated by varying the reaction time, concentration, and carboxylation content of cellulose nanofibers. Cellulose nanofibers were very effective in producing calcium hydroxide nanoparticles with less than 50 nm sizes out of calcium nitrate–sodium hydroxide precipitation reactions. The formation of smaller-size calcium hydroxide nanoparticles is believed to be the result of heterogeneous nucleation and growth of calcium hydroxide particles on cellulose nanofibers.

The liquid-phase nucleated and grown calcium hydroxide nanoparticles were also deposited onto cellulose nanofibers. The resulting calcium hydroxide nanoparticles were carbonized and generated calcite under atmospheric carbon dioxide in an efficient way.

Possible nanoparticle growth mechanisms



Nanolime on cellulose nanofibers



INTRODUCTION

Calcium compounds including calcium hydroxide are used in diverse applications where supplying them in the form of nanosized particles brings unique advantages in their respective applications. Calcium hydroxide is not only an important component of Portland cement but is also used in the conservation of cultural heritage buildings, dental materials, inhibition of ink corrosion of printed papers, and deacidification of wood products.^{1–5} In the case of conservation and repair of building materials, calcium hydroxide nanoparticles penetrate easily into the cracks and damaged zones of mortars and plasters. Their high surface area to volume ratios offer strong reactivity with atmospheric carbon dioxide and bring excellent binding properties.

Several methods have been used for the synthesis of metal, metal oxide, and metal hydroxide nanoparticles in liquid phases. Those can be briefly classified as co-precipitation by synthesis of metals, precipitation of metals by reduction, radiation-assisted reduction, precipitation of oxides, sol–gel processing, reactions in constrained environments (e.g., emulsion systems), templating, and stabilizing the synthesis with polymers.⁶ In the case of calcium hydroxide, nanoparticles with less than 150 nm sizes are synthesized from CaCl_2 at high temperatures (150–170 °C in glycol systems or micro-emulsion systems).^{7,8} Synthesis of $\text{Ca}(\text{OH})_2$ in aqueous systems and in dextran solutions produced particles larger than 250 nm sizes.^{9,10} Other than calcium hydroxide nanoparticles, a novel nanocomposite scaffold is developed

by homogeneous deposition of hydroxyapatite (HAP) on a cellulose nanocrystal (CNC) matrix suspension.^{11,12}

Cellulose nanocrystals and cellulose nanofibers have been investigated for the synthesis of Ag, Au, and Pd metals, mostly to produce hybrid systems for biomedical applications.^{13–15} In this study, carboxylated cellulose nanofibers¹⁶ were used for the first time to synthesize calcium hydroxide nanofibers by co-precipitating from $\text{Ca}(\text{NO}_3)_2$ and NaOH in aqueous solutions at room temperature. The objective of this study was not only to synthesize nanosized calcium hydroxide particles with a facile method but also to shed some light on the co-precipitation process in the presence of cellulose nanofibers.

EXPERIMENTAL SECTION

Materials. Cellulose nanofibers (CNFs) were prepared by using hardwood pulp as a feedstock and applying 2,2,6,6-tetramethylpiperidine-1-oxyl (TEMPO)-mediated oxidation along with mechanical defibrillation.¹⁶ Cellulose nanofibers were lignin- and hemicellulose-free according to chemical analysis. The preparation of the cellulose nanofibers with carboxylate functionalities is given with full descriptions by Saito et al.^{17,18} The carboxylate contents of the oxidized cellulose nanofibers were determined by using a conductivity titration technique.¹⁷ CNF samples were prepared at two levels of carboxylate concentrations: 0.70 and 1.27 mmol/g. They

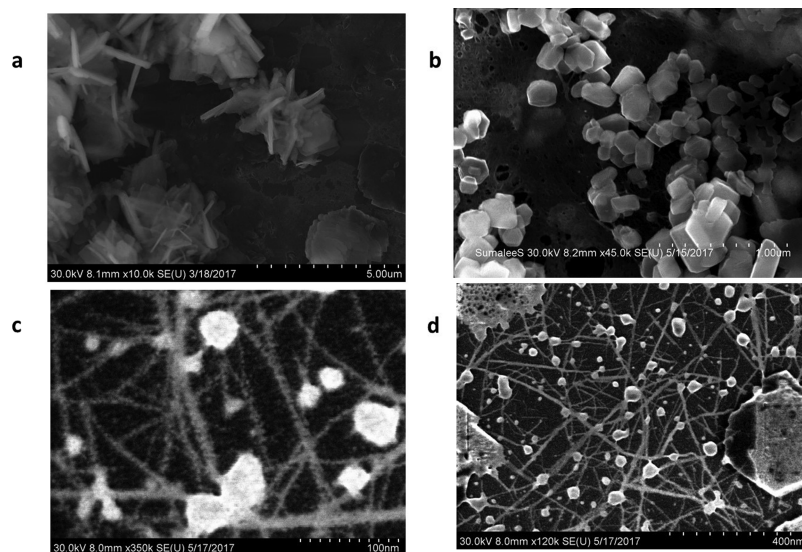
Received: August 16, 2019

Accepted: October 30, 2019

Published: November 25, 2019

Table 1. Reaction Conditions Used for the Precipitation of $\text{Ca}(\text{OH})_2$ in $0.167 \text{ mol}\cdot\text{dm}^{-3} \text{ Ca}(\text{NO}_3)_2$ and $0.167 \text{ mol}\cdot\text{dm}^{-3} \text{ NaOH}$ Mixtures

reaction no.	reaction time (min)	CNF	CNF addition concentration (%)	$[\text{COO}^-]$ on CNF (mmol/g)	CNF in solution ($\text{g}\cdot\text{dm}^{-3}$)	$[\text{COO}^-]$ in solution ($\text{mmol}\cdot\text{dm}^{-3}$)
1	60	0	0	0	0	0
2	60	CNF070	0.1	0.70	0.167	0.117
3	60	CNF070	0.2	0.70	0.333	0.233
4	60	CNF070	0.3	0.70	0.500	0.350
5	60	CNF070	1.0	0.70	1.666	1.167
6	15	CNF127	0.2	1.27	0.333	0.423
7	60	CNF127	0.2	1.27	0.333	0.423

**Figure 1.** SEM of calcium hydroxide particles prepared with mixing $0.167 \text{ mol}\cdot\text{dm}^{-3} \text{ NaOH}$ and $0.167 \text{ mol}\cdot\text{dm}^{-3} \text{ Ca}(\text{NO}_3)_2$ in (a) the absence of CNFs and the presence of (b) $0.167 \text{ g}\cdot\text{dm}^{-3}$ CNF070, (c) $0.333 \text{ g}\cdot\text{dm}^{-3}$ CNF070 with higher magnification, and (d) $0.333 \text{ g}\cdot\text{dm}^{-3}$ CNF070 with lower magnification.

were referred to as CNF070 and CNF127, respectively. Cellulose nanofibers have 500–2000 nm length and 4–6 nm width (Figure S1).

Anhydrous sodium hydroxide $[\text{NaOH}]$ and calcium nitrate tetrahydrate $[\text{Ca}(\text{NO}_3)_2\cdot 4\text{H}_2\text{O}]$ were purchased from Fisher Scientific Canada. Solutions (0.4 M) of $\text{Ca}(\text{NO}_3)_2$ and NaOH solutions were prepared employing deionized water.

Preparation of Nanolime Particles. First, 250 mL of 0.4 M $\text{Ca}(\text{NO}_3)_2$ and 100 mL of CNFs at various fiber and carboxylate concentrations were mixed and stirred for 10 min, and then 250 mL of 0.4 M NaOH was added drop by drop into the CNF suspension in $\text{Ca}(\text{NO}_3)_2$ solution. The color of the CNF suspension turned milky, and the mixture was stirred at 35°C for a period of time. Concentrations of both $\text{Ca}(\text{NO}_3)_2$ and NaOH were $0.167 \text{ mol}\cdot\text{dm}^{-3}$ in the final mixture. To purify the final milky precipitate, several centrifugation and washing steps with deionized water were done to remove NaNO_3 and NaOH . The summary of prepared mixtures is given in Table 1.

After the completion of reactions, samples were washed and centrifuged several times and redispersed in deionized water. Carbonation of $\text{Ca}(\text{OH})_2$ nanoparticles on cellulose nanofibers was evaluated by transferring samples in Petri dishes, letting them dry under natural air convection, and aging them for 90 days.

Characterization of $\text{Ca}(\text{OH})_2$ /CNF Hybrids. The morphologies and sizes of $\text{Ca}(\text{OH})_2$ particles were visually

inspected by SEM using a Hitachi model S-4800 instrument equipped with a field emission source operating at an accelerating voltage of 30 kV. Samples were prepared by using $10 \mu\text{L}$ of redispersed CNF/precipitation reaction mixtures after keeping in deionized water for 24 h. Samples were mounted on a glow-discharged carbon-coated Cu grid. Excess water from samples was taken out, and samples were stained by depositing a drop of uranyl acetate solution (2 wt % in water) on the grid for 5 min. The excess solution was absorbed on filter paper, and the grid was dried at room temperature for 24 h prior to obtaining the images.

FTIR spectra of CNF/precipitation reaction products before and after atmospheric air carbonation were acquired with a Varian FTIR spectrophotometer (FTS-7000) by using freeze-dried samples at room temperature under continuous nitrogen purging. Samples were scanned by using an attenuated total reflection (ATR) technique, and plots of transmission (%) versus wavenumbers were obtained in the range of $4000\text{--}400 \text{ cm}^{-1}$ with a resolution of 4 cm^{-1} by cumulating 32 scans.

The thermal decomposition behavior of CNFs and CNF/precipitation reaction products before and after atmospheric air carbonation was determined by using a thermogravimetric analyzer (TGA 500, TA instrument). Samples (20 mg) were heated with a heating rate of $10^\circ\text{C}/\text{min}$ from 25 up to 1000°C , while the apparatus was continually flushed with a N_2 flow of $40 \text{ mL}/\text{min}$.

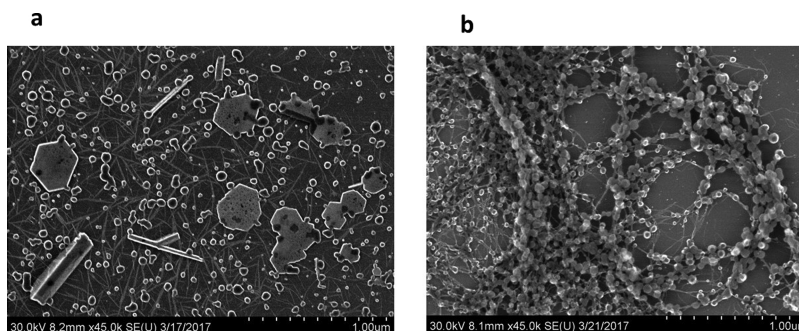


Figure 2. Reaction of $0.167 \text{ mol}\cdot\text{dm}^{-3}$ NaOH and $0.167 \text{ mol}\cdot\text{dm}^{-3}$ $\text{Ca}(\text{NO}_3)_2$ in the presence of $0.333 \text{ g}\cdot\text{dm}^{-3}$ CNF127 with reaction times of (a) 15 min and (b) 60 min.

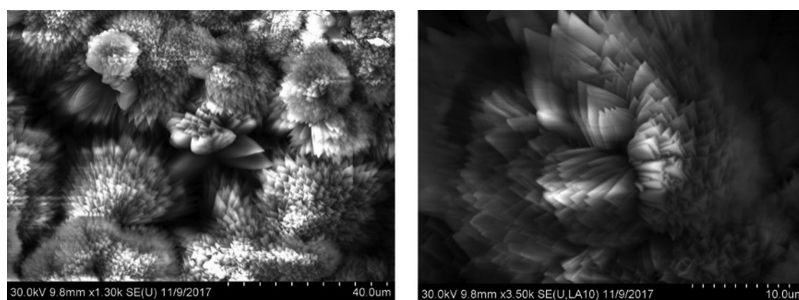
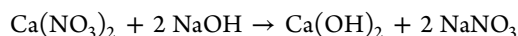


Figure 3. SEM of 90 day-aged calcium hydroxide nanoparticle–CNF hybrid systems, which were prepared by mixing $0.167 \text{ mol}\cdot\text{dm}^{-3}$ NaOH and $0.167 \text{ mol}\cdot\text{dm}^{-3}$ $\text{Ca}(\text{NO}_3)_2$ in the presence of $0.333 \text{ g}\cdot\text{dm}^{-3}$ CNF070 and are shown in two different magnifications.

RESULTS AND DISCUSSION

Hydrated lime (calcium hydroxide) was produced by adding NaOH solution dropwise into the $\text{Ca}(\text{NO}_3)_2$ solutions in CNF suspensions while stirring. The following well-recognized reaction takes place:



Since $\text{Ca}(\text{OH})_2$ is scarcely soluble in water ($k_{\text{sp}} = 5.5 \times 10^{-6}$ and solubility in water is $0.233 \text{ mmol}\cdot\text{dm}^{-3}$ at 20°C), it precipitated under the condition of a high degree of supersaturation (Table 1). The precipitation of $\text{Ca}(\text{OH})_2$ particles without cellulose nanofibers in aqueous solutions resulted in hexagonal prismatic crystals as illustrated in Figure 1a. Individual $\text{Ca}(\text{OH})_2$ particles were relatively uniform with $2 \mu\text{m}$ width and 200 nm length; however, they formed aggregates and precipitated. In the next run, the same precipitation experiment was carried out in the presence of $0.167 \text{ g}\cdot\text{dm}^{-3}$ cellulose nanofibers, which have a 0.70 mmol/g carboxylate concentration on fiber surfaces (CNF070). Smaller calcium hydroxide particles with a width of $100\text{--}200 \text{ nm}$ were generated under these conditions. Individual calcium hydroxide particles were still in a hexagonal prismatic shape, and no visible attachments of calcium hydroxide particles on cellulose nanofibers were observed by SEM in Figure 1b. Those particles were smaller than the ones ($\sim 296 \text{ nm}$) obtained by Samanta et al., which were obtained by applying a similar chemical process with calcium nitrate dihydrate and sodium hydroxide as precursors, however, without the presence of any templates.¹⁰ Increasing the CNF070 concentration in the aqueous phase to $0.333 \text{ g}\cdot\text{dm}^{-3}$ resulted in the deposition of smaller particles with less than 10 nm size onto cellulose nanofiber surfaces (Figure 1c), in addition to bigger ($\sim 50 \text{ nm}$) irregularly shaped particles that were not attached to cellulose nanofibers. Those bigger particles are more visible on the lower-magnification

view in Figure 1d. The XRD pattern of these samples still showed the characteristics of hexagon-shaped portlandite. Hence, the presence of CNFs in the suspension resulted in (1) $\text{Ca}(\text{OH})_2$ particles with particles sizes of around 50 nm , which did not have well-defined shapes and did not attach onto the cellulose nanofibers, and (2) much smaller $\text{Ca}(\text{OH})_2$ particles around cellulose nanofibers. Both of those particles were much smaller than the nanoparticles synthesized from reaction media in glycols ($\sim 100 \text{ nm}$)⁸ and in aqueous ionic and nonionic dextran solutions ($\sim 1000 \text{ nm}$).⁹ The role of cellulose nanofibers was investigated further by increasing the CNF070 concentration in the solution from 0.333 to $1.167 \text{ g}\cdot\text{dm}^{-3}$. Aggregates of much smaller particles and a network of cellulose nanofibers were seen at the CNF suspension with a concentration of $1.667 \text{ g}\cdot\text{dm}^{-3}$ (Figure S2). The carboxylate functional groups on cellulose nanofibers due to TEMPO-mediated oxidation also affected both the size and morphology of $\text{Ca}(\text{OH})_2$ particles. Increasing the carboxylation content of CNFs from 0.70 to 1.27 mmol/g while keeping the CNF concentration in solution constant at $0.333 \text{ g}\cdot\text{dm}^{-3}$ resulted again in a shape change from irregularly shaped particles to pearl-like spherical nanosized $\text{Ca}(\text{OH})_2$ particles. Cellulose nanofibers, CNF127, were all wrapped with calcium hydroxide nanoparticles (Figure S3).

The reaction time for the formation of $\text{Ca}(\text{OH})_2$ had a significant effect on the morphology of particles. Experiments were carried out by reacting $0.167 \text{ mol}\cdot\text{dm}^{-3}$ NaOH with $0.167 \text{ mol}\cdot\text{dm}^{-3}$ $\text{Ca}(\text{NO}_3)_2$ in the presence of $0.167 \text{ g}\cdot\text{dm}^{-3}$ CNF127, which has 1.27 mmol/g carboxylate groups on the CNF surfaces (Figure 2). A reaction time of 15 min resulted in nanometer-sized nonuniform prismatic calcium hydroxide particles mostly unattached onto CNF surfaces in addition to some bigger hexagon-shaped particles. However, increasing the reaction time to 60 min generated pearl-like spherical

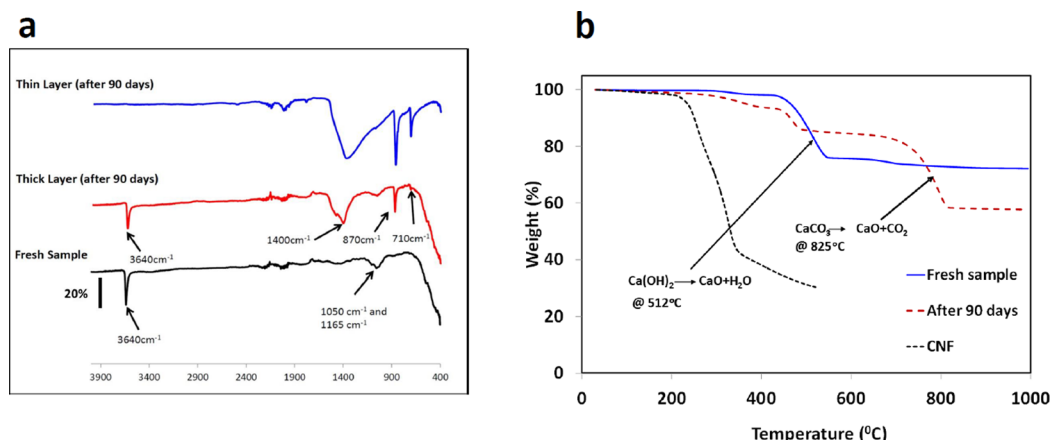


Figure 4. (a) Changes in % transmission FTIR spectra, (b) thermogravimetric analysis plots of a freshly generated $\text{Ca}(\text{OH})_2/\text{CNF}$ hybrid film after 90 days of exposure to air along with CNFs.

nanometer-sized $\text{Ca}(\text{OH})_2$ particles built on the cellulose nanofibers having approximately the same size as the nonuniform prismatic particles observed after 15 min of reaction.

One of the objectives for producing calcium hydroxide nanoparticles is to utilize them as a binder for cultural heritage structures, which heals the cracks of limestones by an effective carbonation process under atmospheric conditions. Therefore, the reaction of the $\text{Ca}(\text{OH})_2/\text{CNF}$ hybrid system with atmospheric carbon dioxide is crucial. The carbonation process of $\text{Ca}(\text{OH})_2$ nanoparticles in the CNF hybrid systems was tested by spreading them as films and aging them under atmospheric conditions for 90 days. Figure 3 shows the SEM picture of a 90 day-aged $\text{Ca}(\text{OH})_2$ nanoparticle/CNF hybrid system, which was obtained by following experimental run 4 listed in Table 1. The carbonation process produced a stable polymorph of calcium carbonate (CaCO_3), calcite.

The FTIR spectra of a freshly synthesized $\text{Ca}(\text{OH})_2/\text{CNF}$ hybrid matrix (obtained by reaction 4) along with their exposure to open air for 90 days from thick and thin dried layers of films are shown in Figure 4a. The fresh sample was almost all $\text{Ca}(\text{OH})_2/\text{CNF}$ hybrid systems with the main strong adsorption peak at 3640 cm^{-1} , which corresponds to OH stretching of $\text{Ca}(\text{OH})_2$, and signature bands at 1050 cm^{-1} from the C–C bond and 1165 cm^{-1} from the C–O–C asymmetrical stretching mode of the cellulose backbone. Exposure of dried $\text{Ca}(\text{OH})_2/\text{CNF}$ hybrid films to atmospheric air resulted in the conversion of $\text{Ca}(\text{OH})_2$ to calcium carbonate with the main CO_3 peaks at 710, 870, and 1400 cm^{-1} . The thin layer of dried $\text{Ca}(\text{OH})_2/\text{CNF}$ hybrid film showed a total conversion of $\text{Ca}(\text{OH})_2$ to CaCO_3 as opposed to a thick layer of dried film, which resulted in only a limited conversion to CaCO_3 . The carbonation was slower in the case of a thick film than a thin film because the cellulose nanofibers delayed the diffusion of atmospheric carbon dioxide through the hybrid $\text{Ca}(\text{OH})_2/\text{CNF}$ film. Figure 4b shows the thermogravimetric analysis of a fresh $\text{Ca}(\text{OH})_2/\text{CNF}$ hybrid system, which was obtained by the reaction 4 (Table 1) procedure and its aging after 90 days under open air along with a CNF sample before the preparation of $\text{Ca}(\text{OH})_2/\text{CNF}$ hybrid materials. As can be seen, in the case of CNFs, cellulose without the presence of any $\text{Ca}(\text{OH})_2$ decomposed over a narrow temperature range, between 280 and $360\text{ }^\circ\text{C}$. This is a very well-defined decomposition temperature range, which is due to cellulose's

very homogeneous semicrystalline structure of linked D-glucose units. The weight loss observed between 100 and $150\text{ }^\circ\text{C}$ in all three samples was due to the loss of residual moisture. In the case of the $\text{Ca}(\text{OH})_2/\text{CNF}$ hybrid material, the moisture loss was $\sim 2.1\%$. The fresh $\text{Ca}(\text{OH})_2/\text{CNF}$ system showed a primary weight loss around $500\text{ }^\circ\text{C}$ due to the decomposition of $\text{Ca}(\text{OH})_2$ to CaO and H_2O at $512\text{ }^\circ\text{C}$. In the case of the 90 day-aged sample, the magnitude of such decomposition decreased drastically at $512\text{ }^\circ\text{C}$, and another major weight loss appeared at $800\text{ }^\circ\text{C}$. It was due to the conversion of $\text{Ca}(\text{OH})_2$ by carbonation to CaCO_3 after 90 days of aging under atmospheric air. Such CaCO_3 decomposed to CaO and CO_2 at $825\text{ }^\circ\text{C}$.

The yield of formation of $\text{Ca}(\text{OH})_2$ nanoparticles based on the added amount of $\text{Ca}(\text{NO}_3)_2$ can be estimated by following the decomposition of fresh $\text{Ca}(\text{OH})_2$ to CaO and H_2O from TGA. The weight loss due to H_2O generation around $512\text{ }^\circ\text{C}$ was 22.17% from the fresh $\text{Ca}(\text{OH})_2/\text{CNF}$ hybrid system in reaction 4. Hence, the amount of $\text{Ca}(\text{OH})_2$ in the $\text{Ca}(\text{OH})_2/\text{CNF}$ hybrid system was 91.2% according to a simple stoichiometric calculation $(22.17 \times \text{MW}_{\text{Ca}(\text{OH})_2}/\text{MW}_{\text{H}_2\text{O}})$. Consequently, the CNF content in the hybrid system was found to be 6.8% after accounting the moisture content of 2.1% . This gives the w/w ratio of $\text{Ca}(\text{OH})_2/\text{CNF}$ to be 13.6 . The stoichiometric amount of $\text{Ca}(\text{OH})_2$ formed was 6.72 g in the reaction pot, which also contains 0.333 g of CNF. Hence, the theoretical w/w ratio of $\text{Ca}(\text{OH})_2/\text{CNF}$ was 18.6 . Therefore, one can calculate the yield of $\text{Ca}(\text{OH})_2$ particles on CNFs to be 73% $(13.6 \times 100/18.6)$. This gave the CNF a surface coverage of $4.5 \times 10^{-14}\text{ g}\cdot\text{mm}^{-2}$ based on a $300\text{ m}^2/\text{g}$ specific surface area of the CNF. X-ray diffraction patterns after aging showed that the calcite (CaCO_3) phase was formed by carbonation of $\text{Ca}(\text{OH})_2$ under atmospheric air and identified as rhombohedral calcite (Figure S4).

Although experiments were limited and the theory of formation of nanoparticles nevertheless was not trivial, results were still used to postulate particle formation mechanisms. The precipitation and formation of calcium hydroxide nanoparticles in the presence of carboxylated cellulose nanofiber suspensions must be discussed by considering the effects of cellulose nanofibers on the nucleation and crystal growth. Cellulose nanofibers can be considered as templates for the precipitation of calcium hydroxide, like the use of cellulose nanocrystals and cellulose nanofibers where Ag and Au metal ions were

precipitated from their precursor metals.¹⁹ The reaction can also be considered as co-precipitation, which involves the direct co-precipitation of Ca^{2+} and OH^- ions in the presence of carboxylated CNF suspensions maintained at basic conditions.⁶ In another way, the precipitation reaction can be considered in a constrained environment due to the cross-linked network formation of cellulose nanofibers.²⁰

The co-precipitation process of calcium hydroxide involves two stages: a short burst of nucleation and growth of nuclei. The nucleation is driven by the degree of supersaturation, $S = C/C_{\text{eq}}$ where C and C_{eq} are the $\text{Ca}(\text{OH})_2$ concentration at saturation and equilibrium. In our case, those were 0.333 and 0.0233 $\text{mol}\cdot\text{dm}^{-3}$, respectively, in the reported experiments. Thus, the driving force for the precipitation was $\Delta C = C - C_{\text{eq}} = 0.310 \text{ mol}\cdot\text{dm}^{-3}$. The rate of nucleation per unit volume, R_N , is proportional to $\exp(1/\ln^2 S)$ if all other reactions are kept constant. In the presence of cellulose nanofibers, the barrier to overcome for nucleation is expected to be further reduced due to nucleation on CNF surfaces. Heterogeneous nucleation depends on the contact angle (θ) of the nucleus on CNF surfaces. Hence, the free energy needed for heterogeneous nucleation (ΔG_{het}) is expressed as the product of homogeneous nucleation (ΔG_{homo}) and a function of contact angle ($f(\theta)$).²¹ For a total nonwetting case ($\theta = 180^\circ$), the nucleus has no affinity for the substrate and no heterogeneous nucleation happens. On the other side, ΔG_{het} approaches zero for a full wetting case ($\theta \rightarrow 0^\circ$). Hence, the buildup of calcium hydroxide nanoparticles suggested that nuclei formation in the bulk liquid phase was drastically lowered, and CNF surfaces acted like heterogeneous nucleation sites. Ca^{2+} cations adsorbed on negatively charged carboxylated CNF surfaces are expected to be ideal sites for the nucleation (Graphical Abstract, Scheme a). As discussed by Cushing et al., there is a slow growth of the nuclei occurring either by a diffusion-controlled or surface reaction-controlled process.⁶ Experimental evidence, such as a decrease in nanoparticle size with an increase in CNF concentration, suggests that the precipitation reaction of calcium hydroxide nanoparticles in CNF suspensions was diffusion-controlled.

Another likely mechanism is the deposition of “liquid-phase nucleated” calcium hydroxide particles onto cellulose nanofibers by colloidal deposition before growing further in the liquid phase. In addition to the adsorption on CNFs, calcium ions also form bridges between the nanofibrils at high NaNO_3 salt concentrations and generate three-dimensional networks.²² In an aqueous environment of high pH, the zeta potentials of calcium hydroxide nanoparticles and carboxylated cellulose nanofibers are around +7¹⁰ and −50 mV, respectively.²³ Hence, colloidal deposition of $\text{Ca}(\text{OH})_2$ nanoparticles onto CNFs is favorable. These conditions most likely favor the colloidal parakinetic deposition of “early-stage-grown” calcium hydroxide nanoparticles onto cellulose nanofibers inside the Ca^{2+} cross-linked networks of cellulose nanofibers (Graphical Abstract, Scheme b).

CONCLUSIONS

Carboxylated cellulose nanofibers in $\text{Ca}(\text{NO}_3)_2$ solutions at room temperature were used for the first time to harvest calcium hydroxide nanoparticles with less than 50 nm particle size and in the form of deposits on the CNF surfaces. The process is simple and solvent-free and did not employ any surface active agent. If desired, $\text{Ca}(\text{OH})_2/\text{CNF}$ hybrid systems can also be used by drying and reintroducing them into

another polar organic solvent such as ethanol or butanol instead of water. In addition, the presence of CNFs in the hybrid system can offer better rheology control if the formation of nanolime films is desired. The resulting calcium hydroxide nanoparticles were effectively carbonized and generated calcite under atmospheric conditions. The formation of smaller-size calcium hydroxide nanoparticles is believed to be the result of more than one mechanism; nevertheless, both of them depend on the adsorption of Ca^{2+} cations onto carboxylated cellulose nanofibers. First of all, adsorption of calcium cations initiate heterogeneous nucleation of CNF surfaces and growth of $\text{Ca}(\text{OH})_2$ particles around fiber surfaces. Second, calcium ions bridge between the nanofibers at high NaNO_3 salt concentrations and generate a three-dimensional network. This condition most likely favors the colloidal deposition of liquid-phase nucleated calcium hydroxide nanoparticles onto cellulose nanofibers inside the Ca^{2+} cross-linked networks of cellulose nanofibers. Further studies are warranted to elucidate and control the formation of nanoparticles with those two mechanisms by investigating the counterions coming from calcium salts, temperature, mixing conditions, and preparation procedures.

ASSOCIATED CONTENT

Supporting Information

The Supporting Information is available free of charge at <https://pubs.acs.org/doi/10.1021/acsomega.9b02643>.

SEM of TEMPO-oxidized nanofibers and effect of CNF concentration on $\text{Ca}(\text{OH})_2/\text{CNF}$ hybrids (Figure S1); effect of carboxylate concentration on $\text{Ca}(\text{OH})_2/\text{CNF}$ hybrids shown with SEM images (Figure S2); X-ray diffraction patterns of $\text{Ca}(\text{OH})_2/\text{CNF}$ obtained by using reaction 4 and after aging under atmospheric air (Figure S3) (PDF)

AUTHOR INFORMATION

Corresponding Author

*E-mail: yaman.boluk@ualberta.ca.

Notes

The authors declare no competing financial interest.

ACKNOWLEDGMENTS

The authors thank the Canada Foundation for Innovation (CFI) for the funding of the pilot-scale cellulose nanofiber unit with Project CFI #29141.

REFERENCES

- (1) Chelazzi, D.; Poggi, G.; Jaidar, Y.; Toccafondi, N.; Giorgi, R.; Baglioni, P. Hydroxide nanoparticles for cultural heritage: consolidation and protection of wall paintings and carbonate materials. *J. Colloid Interface Sci.* **2013**, 392, 42–49.
- (2) Chelazzi, D.; Giorgi, R.; Baglioni, P. Nanotechnology for Vasa Wood De-Acidification. In *Macromolecular symposia*; Wiley Online Library: 2006, pp 30–36.
- (3) Mohammadi, Z.; Dummer, P. M. H. Properties and applications of calcium hydroxide in endodontics and dental traumatology. *Int. Endod. J.* **2011**, 44, 697–730.
- (4) Rodriguez-Navarro, C.; Vettori, I.; Ruiz-Agudo, E. Kinetics and mechanism of calcium hydroxide conversion into calcium alkoxides: Implications in heritage conservation using nanolimes. *Langmuir* **2016**, 32, 5183–5194.

- (5) Rodriguez-Navarro, C.; Suzuki, A.; Ruiz-Agudo, E. Alcohol dispersions of calcium hydroxide nanoparticles for stone conservation. *Langmuir* **2013**, *29*, 11457–11470.
- (6) Cushing, B. L.; Kolesnichenko, V. L.; O'Connor, C. J. Recent advances in the liquid-phase syntheses of inorganic nanoparticles. *Chem. Rev.* **2004**, *104*, 3893–3946.
- (7) Nanni, A.; Dei, L. Ca(OH)₂ nanoparticles from W/O microemulsions. *Langmuir* **2003**, *19*, 933–938.
- (8) Salvadori, B.; Dei, L. Synthesis of Ca(OH)₂ nanoparticles from diols. *Langmuir* **2001**, *17*, 2371–2374.
- (9) Hardikar, V. V.; Matijević, E. Influence of ionic and nonionic dextrans on the formation of calcium hydroxide and calcium carbonate particles. *Colloids Surf., A* **2001**, *186*, 23–31.
- (10) Samanta, A.; Chanda, D. K.; Das, P. S.; Ghosh, J.; Mukhopadhyay, A. K.; Dey, A. Synthesis of nano calcium hydroxide in aqueous medium. *J. Am. Ceram. Soc.* **2016**, *99*, 787–795.
- (11) Huang, C.; Bhagia, S.; Hao, N.; Meng, X.; Liang, L.; Yong, Q.; Ragauskas, A. J. Biomimetic composite scaffold from an in situ hydroxyapatite coating on cellulose nanocrystals. *RSC Adv.* **2019**, *9*, 5786–5793.
- (12) Huang, C.; Hao, N.; Bhagia, S.; Li, M.; Meng, X.; Pu, Y.; Yong, Q.; Ragauskas, A. J. Porous artificial bone scaffold synthesized from a facile in situ hydroxyapatite coating and crosslinking reaction of crystalline nanocellulose. *Materialia* **2018**, *4*, 237–246.
- (13) Chen, M.; Kang, H.; Gong, Y.; Guo, J.; Zhang, H.; Liu, R. Bacterial cellulose supported gold nanoparticles with excellent catalytic properties. *ACS Appl. Mater. Interfaces* **2015**, *7*, 21717–21726.
- (14) Lam, E.; Hrapovic, S.; Majid, E.; Chong, J. H.; Luong, J. H. T. Catalysis using gold nanoparticles decorated on nanocrystalline cellulose. *Nanoscale* **2012**, *4*, 997–1002.
- (15) Incani, V.; Danumah, C.; Boluk, Y. Nanocomposites of nanocrystalline cellulose for enzyme immobilization. *Cellulose* **2013**, *20*, 191–200.
- (16) El Bakkari, M.; Bindiganavile, V.; Goncalves, J.; Boluk, Y. Preparation of cellulose nanofibers by tempo-oxidation of bleached chemi-thermomechanical pulp for cement applications. *Carbohydr. Polym.* **2019**, *203*, 238–245.
- (17) Saito, T.; Isogai, A. TEMPO-mediated oxidation of native cellulose. The effect of oxidation conditions on chemical and crystal structures of the water-insoluble fractions. *Biomacromolecules* **2004**, *5*, 1983–1989.
- (18) Saito, T.; Kimura, S.; Nishiyama, Y.; Isogai, A. Cellulose nanofibers prepared by TEMPO-mediated oxidation of native cellulose. *Biomacromolecules* **2007**, *8*, 2485–2491.
- (19) Islam, M. S.; Chen, L.; Sisler, J.; Tam, K. C. Cellulose Nanocrystal (CNC)–Inorganic Hybrid Systems: Synthesis, Properties and Applications. *J. Mater. Chem. B* **2018**, *6*, 864.
- (20) Laurent, S.; Forge, D.; Port, M.; Roch, A.; Robic, C.; Vander Elst, L.; Muller, R. N. Magnetic iron oxide nanoparticles: synthesis, stabilization, vectorization, physicochemical characterizations, and biological applications. *Chem. Rev.* **2008**, *108*, 2064–2110.
- (21) Thanh, N. T. K.; Maclean, N.; Mahiddine, S. Mechanisms of nucleation and growth of nanoparticles in solution. *Chem. Rev.* **2014**, *114*, 7610–7630.
- (22) Jowkarderis, L.; van de Ven, T. G. M. Rheology of semi-dilute suspensions of carboxylated cellulose nanofibrils. *Carbohydr. Polym.* **2015**, *123*, 416–423.
- (23) Liu, P.; Oksman, K.; Mathew, A. P. Surface adsorption and self-assembly of Cu (II) ions on TEMPO-oxidized cellulose nanofibers in aqueous media. *J. Colloid Interface Sci.* **2016**, *464*, 175–182.